

EVALUATION OF IRON OXIDE DECORATED ON GRAPHENE OXIDE (Fe₃O₄/GO) NANOHYBRID INCORPORATED IN PSF MEMBRANE AT DIFFERENT MOLAR RATIOS FOR CONGO RED REJECTION

Article history

Received
24 August 2016
Received in revised form
24 September 2016
Accepted
31 December 2016

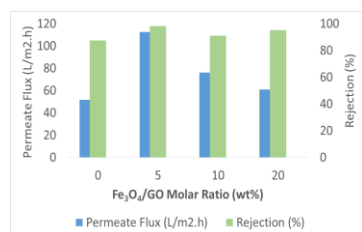
Chai Pui Yun^a, Abdul Wahab Mohammad^{a,b*}, Teow Yeit Haan^{a,b}, Ebrahim Mahmoudi^a

*Corresponding author
drawm@eng.ukm.my

^aDepartment of Chemical and Process Engineering, Faculty of Engineering and Built Environment, Universiti Kebangsaan Malaysia, 43600 Bangi, Selangor Darul Ehsan, Malaysia

^bResearch Centre for Sustainable Process Technology (CESPRO), Faculty of Engineering and Built Environment, Universiti Kebangsaan Malaysia, 43600 Bangi, Selangor Darul Ehsan, Malaysia

Graphical abstract



Abstract

In this study, iron oxide decorated graphene oxide (Fe₃O₄/GO) with three different molar ratio of Fe decorated on GO nanoplates (Fe percentage: 5 wt%, 10wt%, 20 wt%) were synthesized. First, GO nanoplates were synthesized using natural graphite powder according to the Hummers method. Fe₃O₄/GO nanohybrid was then prepared by co-precipitation of FeCl₃.6H₂O and FeSO₄.7H₂O with GO in the presence of ammonia hydroxide (NH₄OH). The nanohybrid was characterized using X-ray diffraction (XRD) and Transmission Electron Microscopy (TEM). The polysulfone (PSf) mixed matrix membranes containing 0.4 wt% of the nanohybrid were prepared by phase inversion method. The effect of different molar ratio of Fe₃O₄/GO nanohybrid on the membrane morphology was examined by several approaches such as porosity & pore size analysis, contact angle, and Field Emission Scanning Electron Microscopy (FESEM) & Energy Dispersive X-Ray (EDX). The mixed-matrix membranes performance were evaluated by measuring the membrane permeate flux and Congo Red (CR) rejection. All the PSf-Fe₃O₄/GO mixed-matrix membrane showed enhanced hydrophilicity, permeate flux and CR rejection compared to the neat PSf membrane. Experiment showed that the PSf-Fe₃O₄/GO mixed-matrix membrane with 5 wt% of Fe decorated onto GO nanoplates was having the best performance with the highest permeate flux of 112.47 L/m².h and the CR rejection of 97±2%.

Keywords: Mixed-Matrix Membrane, Graphene Oxide, Iron Oxide, Polysulfone, Nanohybrid

© 2017 Penerbit UTM Press. All rights reserved

1.0 INTRODUCTION

In the recent years, membrane technology has gained growing attention in the fields of wastewater treatment and reuse, desalination, and drinking

water treatment due to its fascinating stability and efficiency, simple concept and operation, cost effective as well the potential to be scale up in the future [1]. Polymeric membrane is the most used membrane for water treatment due to its easy pore forming mechanism, high flexibility, requires small

space and available at low price [2]. Polysulfone (PSf), is among the common polymer that used for membrane fabrication due to its high stability to chemical resistance and good thermal resistance [3]. However, the performance of PSf membrane is hindered by low resistance to fouling attributed by the hydrophobic nature of PSf [4]. In general, this could possibly reduce the surface wettability of membrane that may generate lower water permeation flux and causing membrane fouling that eventually lead to shorter membrane lifespan [5].

Several studies have been carried out to overcome the drawbacks that hindered the polymeric membrane to perform at its full potential. Among these techniques, blending of inorganic hydrophilic nanofiller into the polymer has attracted the most considerable attention due to its ability to directly improve the hydrophilicity and water permeability [6] as well as controlling the tradeoff between the selectivity and flux of the membrane. There are various hydrophilic nanofillers that have been reported for mixed-matrix membrane fabrication such as TiO₂, ZnO, Fe₃O₄, Ag, Al₂O₃, and SiO₂ [7]. Several studies showed that the presence of nanofiller in membrane polymer could enhance the hydrophilicity of the membrane [8-10]. Although hydrophilic nanofiller could resolve the drawbacks of polymeric membrane, the hydrophilic nanofiller itself has a great tendency to aggregate when blended with hydrophobic polymer solution due to the hydrophobic-hydrophilic interaction. This would give negative effect on membrane morphology and performance in terms of rejection capability, pure water flux and hydrophilicity [11]. Attributed to this, graphene oxide (GO) nanoplates has been introduced to tackle this limitation through decorating the nanofillers onto the GO nanoplates [6, 12]. Numerous oxygen-containing functional groups (e.g. hydroxyl, epoxide, carbonyl and carboxyl groups) on GO nanoplates is offering a great platform for nanofiller dispersion [13] thus producing high effective surface area of the nanofillers with excellent mechanical properties [14, 15]. The concept of decorating nanofiller onto GO nanoplate known as nanohybrid has been seen in various mixed-matrix membrane studies [11, 12, 16, 17]. Considering the advantages of the GO nanoplates, the aggregation of nanofiller is expected to be overcome by decorating it onto GO nanoplates.

In our previous study, a novel PSf-Fe₃O₄/GO mixed-matrix membrane was developed with the incorporation of Fe₃O₄/GO nanohybrid into the PSf polymer in enhancing the membrane hydrophilicity [18]. Extended from the previous study, this research work will investigate the effect of different molar ratio of Fe₃O₄/GO towards the characteristics and performance of PSf-Fe₃O₄/GO mixed-matrix membrane such as rejection capability, permeation flux, pore size and porosity, and hydrophilicity in order to seek for the optimum Fe₃O₄/GO molar ratio that give the optimum results.

2.0 METHODOLOGY

2.1 Materials

GO nanoplates were synthesized using extra pure fine graphite (particle size < 50 µm), sodium nitrate (NaNO₃), potassium permanganate (KMnO₄), sulfuric acid (H₂SO₄) (95-98 wt%), and hydrochloric acid (HCl) supplied by R&M Chemicals, Malaysia. Hydrogen peroxide (H₂O₂) supplied by R&M Chemicals, Malaysia was used as reducing agent to reduce KMnO₄ residual during the GO synthesis. Iron-oxide decorated GO (Fe₃O₄/GO) nanohybrid was synthesized using ferric chloride hexahydrate (FeCl₃.6H₂O) and ferrous sulphate heptahydrate (FeSO₄.7H₂O) purchased from Merck, Germany and Bendosen, Malaysia, respectively. Ammonium hydroxide (NH₄OH) supplied by R&M Chemicals, Malaysia was used as reducing agent during Fe₃O₄/GO nanohybrid synthesis. Asymmetric flat sheet membranes were fabricated using PSf pellets as polymer and N-Methyl-2-pyrrolidone (NMP) as solvent, which obtained from GoodFellow, Malaysia and Merck, Germany, respectively. Congo Red (CR) powder supplied by Merck, Germany was used in preparing the model feed solution for membrane performance evaluation.

2.2 Synthesis of Nanomaterials

2.2.1 Graphene Oxide

GO was synthesized using natural graphite powder according to Hummers method [19, 20]. 5 g of graphite powder, 2.5 g of NaNO₃, and 115 ml of H₂SO₄ were mixed together in a round flask. The mixture was then stirred for 30 minutes in an ice bath at the temperature of 0-10 °C. Next, 15 g of KMnO₄ was added gradually into the mixture under continuous stirring. The mixture was allowed to react at the temperature below 10°C for 2 hours and successively stirred at 35°C for another 1 hour. The mixture was then diluted with 230 ml of deionized water while temperature was kept between 25-80 °C. The solution was stirred for another one hour followed by further dilution with deionized water. 10 ml of H₂O₂ was then added into the mixture to reduce the KMnO₄ residual until the colour of the mixture turned into brilliant yellow. Finally, the mixture was centrifuged and rinsed with hydrochloric acid (HCl) aqueous solution before put in freeze dryer to obtain fine brown GO powder.

2.2.2 Fe₃O₄/GO Nanohybrid

Fe₃O₄/GO nanohybrid was synthesized by co-precipitation of FeCl₃.6H₂O and FeSO₄.7H₂O in the presence of GO. First, 1 g of GO was stirred and ultrasonicated in a mixture of deionized water and absolute ethanol. Simultaneously, FeCl₃.6H₂O and FeSO₄.7H₂O were weighted separately in a molar

ratio of 3:1 and stirred in a mixture of deionized water and absolute ethanol to obtain homogeneous solution before adding into GO aqueous solution. The preparation $\text{Fe}_3\text{O}_4/\text{GO}$ nanohybrid was synthesized according to different amount of Fe percentage in GO which was set to be 5 wt%, 10 wt%, and 20 wt%. The temperature of the mixing solution was raised to 60-70 °C and NH_4OH was added gradually to increase the pH to 11. The mixture was allowed to react for 2 hours before cooled down to room temperature. Repeating washing process was carried out using ultrapure water until the pH of the resulting solution reach 7 ± 0.2 . Final washing was done with absolute ethanol. The resulting product was then dried overnight in an oven at 90-100 °C.

2.3 Fabrication of PSf- $\text{Fe}_3\text{O}_4/\text{GO}$ Mixed-Matrix Membrane

Phase inversion method was used for the fabrication of PSf- $\text{Fe}_3\text{O}_4/\text{GO}$ mixed-matrix membrane. The membrane casting solution was prepared by dissolving pre-dried PSf into NMP solvent at the weight composition of 15:85. First, $\text{Fe}_3\text{O}_4/\text{GO}$ nanohybrid was ultra-sonicated in NMP solution for 30 minutes followed with overnight stirring to obtain a homogeneous solution. PSf was dissolved in NMP and subjected to an initial stirring of 100 rpm at 65 °C for 4 hours and 30 minutes to form a homogeneous solution. The homogeneous solution was then left overnight under stirring at 40 °C. Next, homogeneous $\text{Fe}_3\text{O}_4/\text{GO}$ nanohybrid solution with different loading was injected into the PSf/NMP aqueous solution. The produced membrane casting solution was ultra-sonicated for another 30 minutes and kept in dark overnight to remove the trapped air bubbles [21].

The casting solution was cast manually on a clean glass plate using the Filmographe Doctor Blade 360099003 (Braive Instrument, Germany) at a thickness of 0.2 mm. The nascent membrane on the glass plate was then solidified by immediately immersed into ultrapure water at room temperature. The immersion was left for a day to ensure complete solidification.

Table 1 The amount of Fe percentage decorated onto GO nanoplates and the ratio of PSf: NMP: $\text{Fe}_3\text{O}_4/\text{GO}$ nanohybrid in each membrane formulation

Membrane	Amount of Fe percentage decorated onto GO Nanoplates (%)	Ratio of PSf:NMP: $\text{Fe}_3\text{O}_4/\text{GO}$ Nanohybrid
M0 (Neat)	0	3:17:0.00
M5	5	3:17:0.08
M10	10	3:17:0.08
M20	20	3:17:0.08

All the membranes were prepared by doping 0.4 wt% $\text{Fe}_3\text{O}_4/\text{GO}$ nanohybrid (based on the weight of PSf) with different amount of Fe percentage in GO nanoplates as mentioned previously (5 wt%, 10 wt%, and 20 wt%) to investigate the effect of different $\text{Fe}_3\text{O}_4/\text{GO}$ nanohybrid molar ratio on membrane performance. Table 1 showed the weight percent of $\text{Fe}_3\text{O}_4/\text{GO}$ nanohybrid and the ratio of PSf:NMP: $\text{Fe}_3\text{O}_4/\text{GO}$ nanohybrid for each membrane formulation.

2.4 $\text{Fe}_3\text{O}_4/\text{GO}$ Nanohybrid Characterization

2.4.1 X-ray Diffraction (XRD)

XRD technique was used to identify the structure phase and crystal size of the synthesized $\text{Fe}_3\text{O}_4/\text{GO}$ nanohybrid. The XRD analysis was performed by BRUKER AXS D8 ADVANCE diffraction meter (Bruker AXS, GmbH, USA). The system was equipped with a $\text{CuK}\alpha$ radiation ($\lambda = 1.5406 \text{ \AA}$) with scanning in range of 5-80° for 2θ angle. The average crystal size, D was estimated using the Scherrer equation:

$$D = K\lambda / \beta \cos\theta \quad (1)$$

where β is the peak width at half maximum (radian), K is the Scherrer constant ($K = 0.89$), λ is the X-ray wavelength ($\lambda = 1.5406 \text{ \AA}$), and θ is the Bragg diffraction angle (θ).

2.4.2 Transmission Electron Microscope (TEM)

The particle size of Fe_3O_4 was evaluated using the TEM CM-12, (Philips, Netherlands). For the TEM observation, $\text{Fe}_3\text{O}_4/\text{GO}$ nanohybrid suspension was pipetted out and dropped on a 3 mm diameter, 400 mesh carbon-coated grid. The droplet was then wicked to dryness for 10 min before undergoing for TEM imaging at 60 k \times magnification.

2.5 Membrane Characterization

2.5.1 Porosity and Pore Size Estimation

Porosity (ϵ) and pore size (r_m) of the fabricated membranes were determined by the gravimetric method as defined by Eq (2) and Guerout-Elford-Ferry equation, Eq (3), respectively [22, 23].

$$\epsilon = (\omega_1 - \omega_2) / (A \times l \times \rho) \quad (2)$$

$$r_m = \sqrt{(2.9 - 1.75\epsilon) \eta l Q / (\epsilon \times A \times \Delta P)} \quad (3)$$

where ω_1 (kg) is the wet membrane weight, ω_2 (kg) is the dried membrane weight, A (m^2) is the surface area of the membrane, l is the thickness of the membrane (m), ρ is the water density (998 kg/m^3), η is the water viscosity ($8.9 \times 10^{-4} \text{ Pa s}$), Q is the volume of permeated pure water per unit time (m^3/s), and ΔP is the operating pressure (0.1 MPa).

2.5.2 Contact Angle

The membrane wettability was characterized by the static contact angle of the membrane surface, which was measured based on the sessile drop technique using a Drop Shape Analysis System goniometer, model DSA100, (Kruss GmbH, Germany). The membrane sample was cut into an appropriate size and stuck onto a glass slide using double-sided tape. A droplet of deionized water was dropped onto the dry membrane surface with micro-syringe. The micrograph of the contact angle was captured and evaluated using the Drop Shape Analysis software. The reported contact angle was the average of three measurements taken at different locations on the membrane.

2.5.3 Field Emission Scanning Electron Microscopy (FESEM) and Energy Dispersive X-Ray (EDX)

FESEM Merlin Compact (Zeiss, Germany) was used to examine the surface and cross sectional structures of the fabricated membranes. Prior the FESEM analysis, membrane samples were cut into an appropriate size and mounted on the sample holder. Rotary-pumped coating system, Quorum, Q150R S, (Quorum Technologies, Germany) was used to coat the outer surface of the membrane samples with a thin layer of platinum under vacuum to provide electrical conductivity. After platinum sputtering, the membrane samples were examined under the electron microscope. Using the same sample in FESEM, the quality of dispersion and existence of Fe on the membrane surface was examined using FESEM equipped with an EDX spectroscopy under magnification of 500 ×.

2.5.4 Zeta Potential

The surface charge of the fabricated membrane was assessed by zeta potential measurement using Malvern Zeta Sizer Nano ZS (Malvern Instruments, UK). By applying a field strength of 25 V/cm, the zeta potential of membrane surface in 0.1 mM NaCl at pH 7 was measured using 300-350 nm latex particles as the tracer particle (DTS1235 Malvern, UK).

2.6 Membrane Performance

2.6.1 Permeation Flux and Congo Red Rejection

Permeation test was carried out using a stirred cell filtration system (Sterlitech TM HP4750, USA) with an effective membrane area of 14.60 cm². Before the experiment was carried out, the fabricated membrane was compressed at constant pressure of 5 bar for 30 minutes with deionized water to obtain stable permeate flux. 20 ppm CR solution was used as the feed solution during membrane performance study at 1 bar of filtration pressure and 400 rpm stirring speed. Permeation flux was determined according to Eq (4).

$$F=V/At \quad (4)$$

where F is the permeation flux (L/m².h), V is the permeate volume (L), A is the effective membrane area (m²), and t is time (hour). The CR solution concentrations were evaluated by measuring the absorbance of CR using UV-vis spectrophotometer at the wavelength of 497 nm. The CR rejection was then calculated from the difference between feed and permeate concentration according to Eq (5).

$$R (\%) = (1 - C_p/C_f) \times 100\% \quad (5)$$

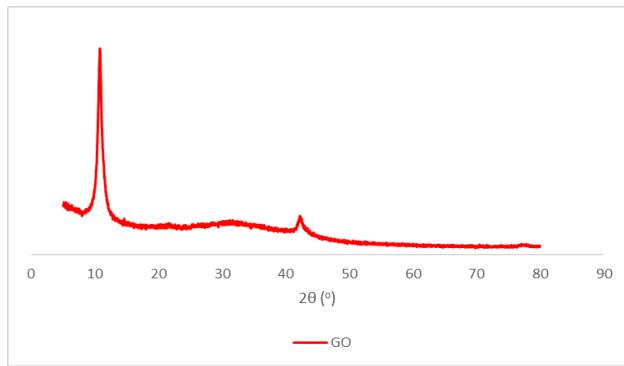
where R is the rejection percentage of CR (%), C_p is the concentration of the permeate solution (mg/l) and C_f is the concentration of the feed solution (mg/l).

3.0 RESULTS AND DISCUSSION

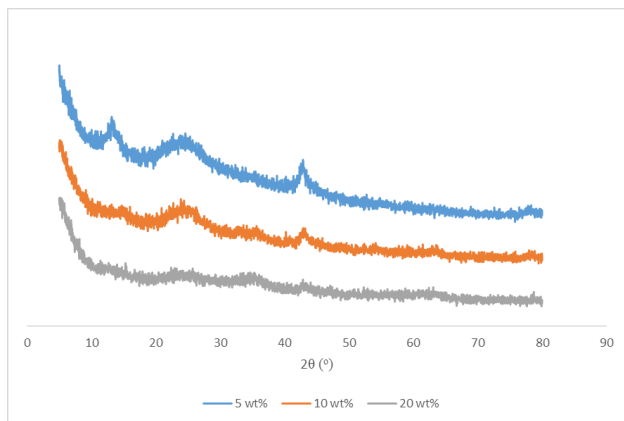
3.1 Fe₃O₄/GO Nanohybrid Characterization

3.1.1 X-ray Diffraction (XRD)

The crystal structures of GO nanoplate and Fe₃O₄/GO nanohybrid were examined using XRD analysis and the XRD patterns of these nanomaterials were shown in Figure 1 (a) and Figure 1(b) respectively. As elucidated by Figure 1 (a), the characteristic peaks of GO nanoplate were observed at 10.80° and 42.22°. The existence of these two significant characteristic peaks indicated the successful oxidation of graphite flakes into GO as reported by other study [24]. On the other hand, the diffraction peaks of all Fe₃O₄/GO nanohybrids were observed to be located at 13.37°, 23.71°, and 43.31° as shown in Figure 1 (b). The peak of 13.37° might refer to the characteristic peak of GO which originally located at 10.80°. The shift indicated that there is interaction between the Fe and the GO nanoplates [25]. Whereas, the characteristic peaks at 23.71° and 43.31° were refer to the reduction of GO (rGO) during heating process [26]. However, there was no obvious peak observed in Fe₃O₄/GO nanohybrid XRD pattern indicated the existence of iron (Fe). This might due to low concentration of Fe used in decorating the GO nanoplate. Similar result was obtained and reported by Kassaei *et al.* (2011) [27]. As the percentage of Fe was increased from 5 wt% to 20 wt%, the diffraction peak (13.37°) that correspond to interaction of Fe-GO become weaker, that could possibly due to decreased of GO content [28].



(a)

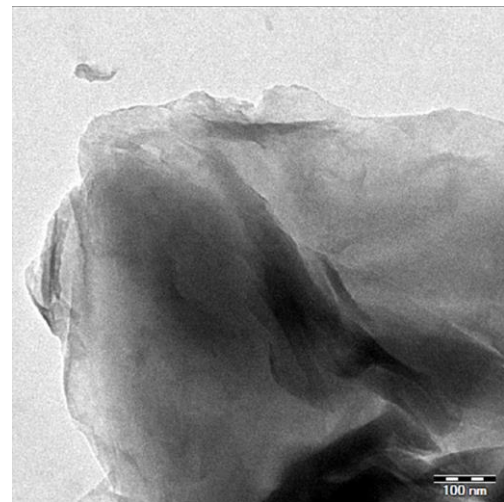


(b)

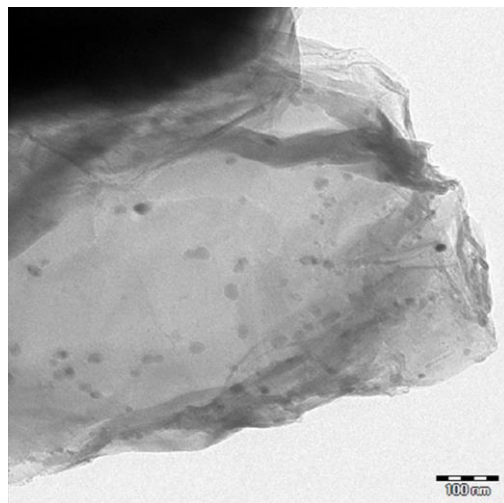
Figure 1 XRD diffraction peak for (a) GO nanoplates and, (b) $\text{Fe}_3\text{O}_4/\text{GO}$ nanohybrid with different molar ratio

3.1.2 Transmission Electron Microscope (TEM)

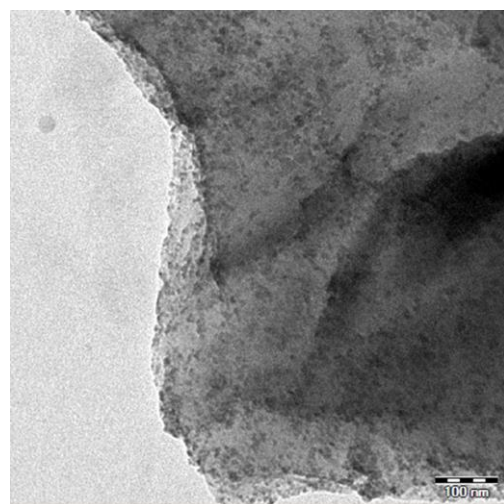
TEM analysis was performed to observe the morphology of GO nanoplates and $\text{Fe}_3\text{O}_4/\text{GO}$ nanohybrids, as well as the distribution pattern of the Fe_3O_4 NPs in $\text{Fe}_3\text{O}_4/\text{GO}$ nanohybrid. The TEM images of GO nanoplates, $\text{Fe}_3\text{O}_4/\text{GO}$ nanohybrid (5wt%), $\text{Fe}_3\text{O}_4/\text{GO}$ nanohybrid (10wt%) and $\text{Fe}_3\text{O}_4/\text{GO}$ nanohybrid (20wt%) was shown in Figure 2 (a), (b), (c), (d) respectively. By comparing the GO nanoplates and the $\text{Fe}_3\text{O}_4/\text{GO}$ nanohybrids, it can be seen that Fe_3O_4 NPs (represented by black spot) was successfully incorporated into GO nanoplates during the synthesis process in producing the $\text{Fe}_3\text{O}_4/\text{GO}$ nanohybrid. It is also can be seen that, as the amount of Fe was increased from 5wt% to 20wt%, the TEM images showed a proportional increased in the density of Fe_3O_4 NPs decorated on GO nanoplates. The TEM images also revealed that almost spherical shape of Fe_3O_4 NPs was decorated into the GO nanoplates. Based on the TEM images, it was hypothesized that Fe_3O_4 NPs was uniformly decorated into GO nanoplates. This is because no significant black aggregation spot was observed.



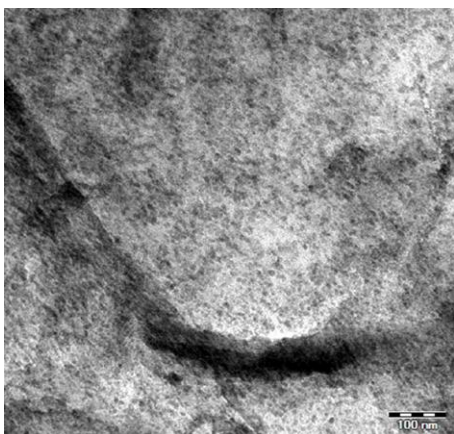
(a) GO



(b) 5 wt%



(c) 10wt%



(d) 20wt%

Figure 2 TEM images of (a) GO, (b) Fe₃O₄/GO (5 wt%), (c) Fe₃O₄/GO (10 wt%) and, (d) Fe₃O₄/GO (20 wt%)

3.2 Membrane Characterization

3.2.1 Pore Size and Porosity

Pore size and porosity analysis are important as it directly related to rejection capability and permeation flux of the membrane. Generally, porosity of the membrane depends on the rate of mass transfer between solvent and non-solvent phase during phase inversion process. The results of the pore size and porosity measurements for different percentage of Fe at constant concentration of 0.4 wt% are given in Table 2. Based on Table 2, an increase of membrane porosity was observed for M5 membrane as compared to the M0 membrane. This is because the presence of hydrophilic functional groups in Fe₃O₄/GO nanohybrid will accelerate the membrane formation by speeding up the exchange rate between solvent and non-solvent phase, thus promoting the pores formation [3]. However, higher percentage of Fe (10 wt% and 20 wt%) decorated onto GO nanoplate resulted in a slightly lower porosity when compared to M0 neat membrane. This phenomenon could be related to the increase amount of Fe percentage in the GO nanoplates. As seen in TEM images, when the percentage of Fe was increased to 10 wt% and 20 wt%, most of the surface of GO nanoplate was occupied by the Fe₃O₄ NPs. These higher density of Fe percentage in the GO nanoplate are postulated to have higher aggregation rate that could cause lower porosity.

The pore size of fabricated neat and Fe₃O₄/GO mixed-matrix membranes were calculated using Eq (2) and the results are tabulated in Table 2. As can be seen in Table 2, the pore size M0, M5, M10, and M20 was 0.0306, 0.0331, 0.0371, and 0.0369 μm , respectively. It can be observed that the pore size of the all the Fe₃O₄/GO mixed-matrix membranes with Fe₃O₄/GO nanohybrid were having relatively larger pore size compared to the neat membrane. The pore enlargement was due to increase of mass

transfer rate between the solvent and non-solvent phase during the phase inversion process that interfere by hydrophilic nanohybrid [29]. Consequently, Fe₃O₄/GO mixed-matrix membranes with bigger pores were induced.

Table 2 Porosity and pore size analysis of each membrane

Membrane	Porosity (%)	Pore size (μm)
M0	56.89	0.0331 \pm 0.0026
M5	76.35	0.0347 \pm 0.0035
M10	62.52	0.0365 \pm 0.0019
M20	59.02	0.0364 \pm 0.0007

3.2.2 Contact Angle

Wettability of the membranes was determined by contact angle measurement. In general, the lower the contact angle, the more hydrophilic the membrane will be. The contact angle of the neat membrane and Fe₃O₄/GO mixed-matrix membranes are shown in Figure 3. It can be seen in Figure 3 that, the contact angle decreased for all molar ratios of Fe₃O₄/GO nanohybrid. The decrement in contact angle could be explained by the reduced interface energy during phase inversion process due to spontaneous migration of hydrophilic Fe₃O₄/GO nanohybrid to the membrane/water interface [30]. From Figure 3, M5 mixed-matrix membrane has the lowest contact angle value at 69.97 $^\circ$ as compared to M0 (78.80 $^\circ$), M10 (71.57 $^\circ$), and M20 (70.73 $^\circ$) membrane indicating that M5 mixed-matrix membrane have the highest hydrophilicity among all membranes.

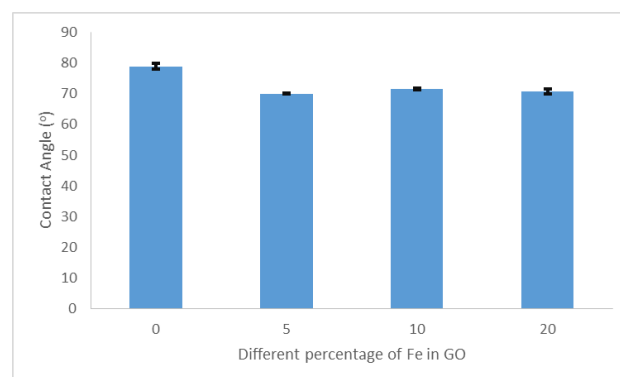


Figure 3 Contact angle of membranes at different molar ratio of Fe in GO

3.2.3 Field Emission Scanning Electron Microscopy (FESEM) and Energy Dispersive X-Ray (EDX)

Figure 4 (a), (b), (c) and (d) show the cross-section FESEM images of M0, M5, M10 and M20 membranes at magnification of 5 k \times . By referring to Figure 4, there is no significant change in the structural of the mixed-matrix membranes as compared to the neat membrane. As could be seen from the FESEM images

in Figure 4, all the membranes displayed fingerlike pore structures. However, there are no trace of nanohybrid can be seen in M5, M10, and M20 mixed-matrix membrane. Such phenomenon had also been observed by other literature studies [30, 31]. However, it does not mean that $\text{Fe}_3\text{O}_4/\text{GO}$ nanohybrid was absence in the mixed-matrix membranes.

The presence of Fe_3O_4 NPs in the membrane matrix was further confirmed and the chemical analysis was performed with FESEM samples for EDX mapping. M5 mixed-matrix membrane was selected to perform the EDX mapping analysis as M5 mixed-matrix membrane was shown to have the least changes of physical structure with the highest porosity and hydrophilicity, and improved pore size compared to M0 neat membrane. Figure 5 (b) represents the EDX mapping of M5 mixed-matrix membrane surface for FESEM micrograph at magnification of $2 \times$ as shown in Figure 5 (a). It could be clearly seen in Figure 5 (b) that Fe_3O_4 NPs which represented by purple colour spot was dispersed uniformly into the membrane matrix.

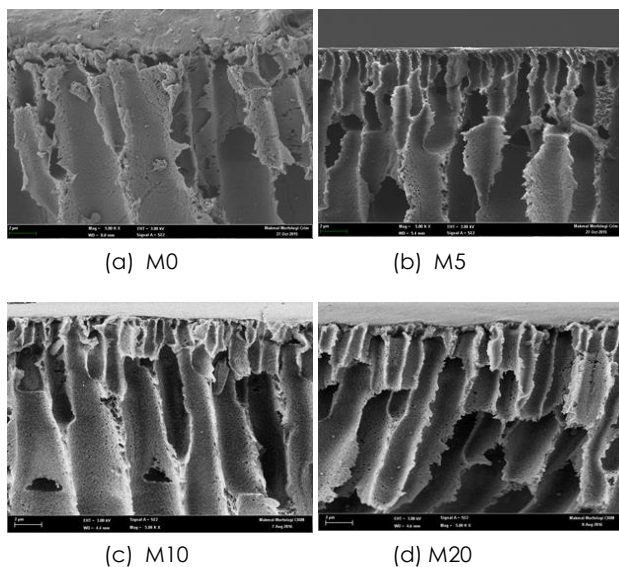


Figure 4 Cross-section FESEM images of fabricated membrane (a) M0, (b) M5, (c) M10 and, (d) M20 at magnification of $5 \times$

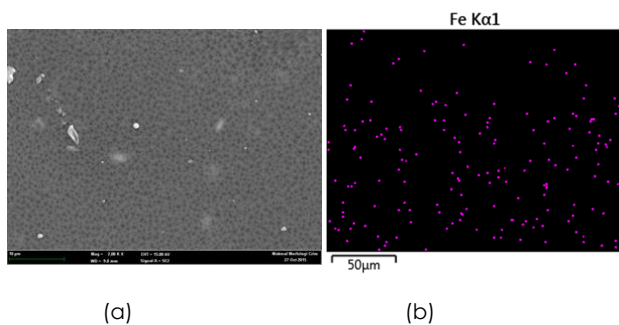


Figure 5 EDX analysis of M5 mixed-matrix membrane (a) FESEM image of M5, (b) EDX Mapping of M5

3.2.4 Zeta Potential

The surface charge of a membrane was measured in terms of surface zeta potential. Figure 6 shows the membrane surface zeta potential of the fabricated membranes with different molar ratios of $\text{Fe}_3\text{O}_4/\text{GO}$ nanohybrid. Result shows that by incorporating nanohybrid into membrane matrices will result in increase of membrane surface charge. From Figure 6, it can be seen that the membrane surface charge of M0 membrane was around -4 ± 5.5 mV. Figure 6 also showed that by incorporating different molar ratio of $\text{Fe}_3\text{O}_4/\text{GO}$ nanohybrid, the membrane surface charge of M5, M10, and M20 mixed-matrix membrane increased to -29 ± 3 mV. Such phenomenon was also observed in other literature study whereby the membrane surface charge of neat PSf membrane was measured to be around -12 mV [32] while the modified membranes are believe to possess higher negative surface charge because of the negatively charged nature of GO powder.

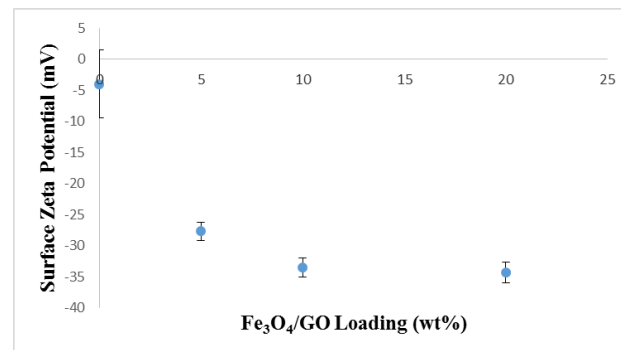


Figure 6 Membrane surface charge of fabricated membrane

3.3 Membrane Performance Evaluation

The permeation flux of all membranes was measured at 1 bar and the results are shown in Figure 7. As can be seen from Figure 7, all the mixed-matrix membrane (M5, M10, and M20) are having higher permeation flux compared to M0 neat membrane. In this study, the maximum permeation flux was obtained when 5wt% molar ratio of $\text{Fe}_3\text{O}_4/\text{GO}$ nanohybrid was doped into the polymer solution. The enhancement of M5 mixed-matrix membrane permeation flux was increased from $51.82 \text{ L/m}^2 \text{ h}$ (M0 neat membrane) to $112.47 \text{ L/m}^2 \text{ h}$ which is two times higher. This could be attributed to the incorporation of hydrophilic $\text{Fe}_3\text{O}_4/\text{GO}$ nanohybrid into the membrane matrix. This postulation was supported by the contact angle result in previous Section 3.2.2 in which the membrane contact angle was decreased with the presence of $\text{Fe}_3\text{O}_4/\text{GO}$ nanohybrid due to the enhancement of membrane hydrophilicity. M5 mixed-matrix membrane that possess high hydrophilicity will therefore promoted the interaction between membrane surface and water molecules and facilitating the permeation of water through the

membrane and resulted in higher permeate flux [4]. Also, the permeate flux for M10 and M20 mixed-matrix membrane with higher density of Fe_3O_4 is lower than the lower density of Fe_3O_4 . This indicate that higher amounts of graphene oxide provide a better dispersion and reduction in aggregation [28]. This could also supported by the porosity result shown in Table 2. As shown in Table 2, the porosity decreased from M5 to M20 mixed-matrix membrane resulted in a proportional decreased of the permeate flux of the respective membranes.

On the other hand, Figure 7 also depicted the rejection capability of M0, M5, M10, and M20 membranes in removing CR. As shown in Figure 7, all the mixed-matrix membranes (M5, M10, and M20) achieved higher rejection percentage in removing CR as compared to M0 membrane. Although the membrane pore size of M0 membrane was relatively smaller than the M5, M10, and M20 mixed-matrix membranes, M5, M10, and M20 mixed-matrix membranes turned out to have higher rejection of CR. This could be attributed to the difference in membrane surface charge of the membranes as mentioned in Section 3.2.4. The increased of membrane surface negative enhancing the electrostatic repulsion between the membrane and CR molecules which was also having a negative zeta potential of -25 ± 3 (mV). This was thus resulted in higher CR rejection for all mixed-matrix membranes as compared to the neat membrane. Moreover, the electrostatic repulsion created between the membrane and CR molecules will possibly impede the attachment of CR molecules onto the membrane surface consequently reduced occasion of membrane fouling.

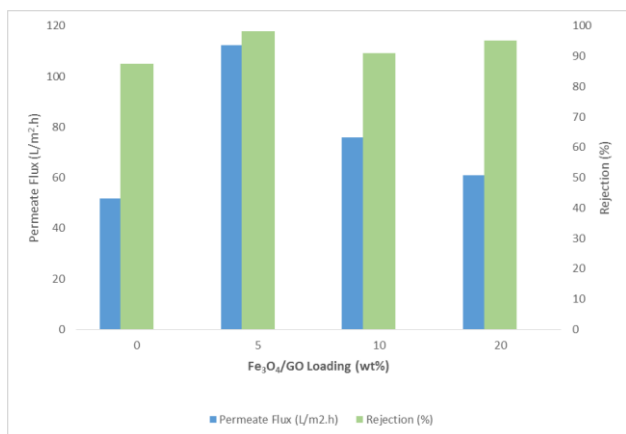


Figure 7 Permeate flux (L/m².h) and rejection (%) of each membranes

4.0 CONCLUSION

PSf- Fe_3O_4 /GO mixed-matrix membranes were successfully fabricated using phase inversion method. It was found that the GO nanoheets has provide a platform for uniform Fe_3O_4 NPs dispersion

prior incorporated into the membrane. Results showed that the fabricated mixed-matrix membranes incorporated with Fe_3O_4 /GO nanohybrid had similar morphologies to the neat membrane. This is mainly attributed to the well distribution of Fe_3O_4 NPs which lessen the drawbacks and limitations of Fe_3O_4 NPs agglomeration problem in the past studies. The M5 mixed-matrix membrane that modified with 0.4 wt% of Fe_3O_4 /GO nanohybrid with 5 wt% molar ratio of Fe_3O_4 was found to have the highest hydrophilicity, permeation flux, and rejection capability. M5 membrane with 0.4 wt% Fe_3O_4 /GO nanohybrid loading was having 112.47 L/m² h of permeate flux and CR rejection as high as $97\% \pm 2$.

Acknowledgement

The authors wish to gratefully acknowledge the financial support for this work by grant NPRP 5-1425-2-607. The Ministry of Education Malaysia is acknowledged for sponsoring P.V. Chai postgraduate study via MyBrain. In addition, the authors wish to acknowledge the CRIM (Centre for Research and Instrumentation Management, UKM) for XRD, XPS, FESEM, and TEM analyses.

References

- [1] Aditya Kiran, S., Y. Lukka Thuyavan, G. Arthanareeswaran, T. Matsuura, and A. F. Ismail. 2016. Impact of Graphene Oxide Embedded Polyethersulfone Membranes for the Effective Treatment of Distillery Effluent. *Chemical Engineering Journal*. 286: 528-537.
- [2] Yin, J., and B. Deng. 2015. Polymer-Matrix Nanocomposite Membranes for Water Treatment. *Journal of Membrane Science*. 479: 256-275.
- [3] Lee, J., H.-R. Chae, Y.J. Won, K. Lee, C.-H. Lee, H.H. Lee, I.-C. Kim, and J.-m. Lee. 2013. Graphene Oxide Nanoplatelets Composite Membrane with Hydrophilic and Antifouling Properties for Wastewater Treatment. *Journal of Membrane Science*. 448: 223-230.
- [4] Ganesh, B. M., A. M. Isloor, and A. F. Ismail. 2013. Enhanced Hydrophilicity and Salt Rejection Study of Graphene Oxide-Polysulfone Mixed Matrix Membrane. *Desalination*. 313: 199-207.
- [5] Ionita, M., A. M. Pandele, L. Crica, and L. Pilan. 2014. Improving the Thermal and Mechanical Properties of Polysulfone by Incorporation of Graphene Oxide. *Composites Part B: Engineering*. 59: 133-139.
- [6] Vatanpour, V., S. S. Madaeni, R. Moradian, S. Zinadini, and B. Astinchap. 2012. Novel Antibifouling Nanofiltration Polyethersulfone Membrane Fabricated from Embedding TiO_2 Coated Multiwalled Carbon Nanotubes. *Separation and Purification Technology*. 90: 69-82.
- [7] Ng, L. Y., A. W. Mohammad, C. P. Leo, and N. Hilal. 2013. Polymeric Membranes Incorporated with Metal/Metal Oxide Nanoparticles: A Comprehensive Review. *Desalination*. 308: 15-33.
- [8] Huang, Z.-Q., F. Zheng, Z. Zhang, H.-T. Xu, and K.-M. Zhou. 2012. The Performance of the PVDF- Fe_3O_4 Ultrafiltration Membrane and the Effect of a Parallel Magnetic Field used during the Membrane Formation. *Desalination*. 292: 64-72.
- [9] Ghaemi, N., S.S. Madaeni, P. Daraei, H. Rajabi, S. Zinadini, A. Alizadeh, R. Heydari, M. Beygzadeh, and S.

- Ghouzivand. 2015. Polyethersulfone Membrane Enhanced with Iron Oxide Nanoparticles for Copper Removal from Water: Application of New Functionalized Fe₃O₄ Nanoparticles. *Chemical Engineering Journal*. 263: 101-112.
- [10] Daraei, P., S. S. Madaeni, N. Ghaemi, E. Salehi, M. A. Khadivi, R. Moradian, and B. Astinchap. 2012. Novel Polyethersulfone Nanocomposite Membrane Prepared by PANI/Fe₃O₄ Nanoparticles with Enhanced Performance for Cu(II) Removal from Water. *Journal of Membrane Science*. 415-416: 250-259.
- [11] Safarpour, M., V. Vatanpour, and A. Khataee. 2015. Preparation and Characterization of Graphene Oxide/TiO₂ Blended PES Nanofiltration Membrane with Improved Antifouling and Separation Performance. *Desalination*. 393: 65-78.
- [12] Wu, H., B. Tang, and P. Wu. 2014. Development of Novel SiO₂-GO Nanohybrid/Polysulfone Membrane with Enhanced Performance. *Journal of Membrane Science*. 451: 94-102.
- [13] Cao, K., Z. Jiang, J. Zhao, C. Zhao, C. Gao, F. Pan, B. Wang, X. Cao, and J. Yang. 2014. Enhanced Water Permeation through Sodium Alginate Membranes by Incorporating Graphene Oxides. *Journal of Membrane Science*. 469: 272-283.
- [14] Zhao, C., X. Xu, J. Chen, and F. Yang. 2013. Effect of Graphene Oxide Concentration on the Morphologies and Antifouling Properties of PVDF Ultrafiltration Membranes. *Journal of Environmental Chemical Engineering*. 1(3): 349-354.
- [15] Zhao, C., X. Xu, J. Chen, G. Wang, and F. Yang. 2014. Highly Effective Antifouling Performance of PVDF/Graphene Oxide Composite Membrane in Membrane Bioreactor (MBR) System. *Desalination*. 340: 59-66.
- [16] Vatanpour, V., A. Shockravi, H. Zarrabi, Z. Nikjavan, and A. Javadi. 2015. Fabrication and Characterization of Anti-Fouling and Anti-Bacterial Ag-Loaded Graphene Oxide/Polyethersulfone Mixed Matrix Membrane. *Journal of Industrial and Engineering Chemistry*. 30: 342-352.
- [17] Koushkbaghi, S., P. Jafari, J. Rabiei, M. Irani, and M. Aliabadi. 2016. Fabrication of PET/PAN/GO/Fe₃O₄ Nanofibrous Membrane for the Removal of Pb(II) and Cr(VI) Ions. *Chemical Engineering Journal*. 301: 42-50.
- [18] Chai, P. V., E. Mahmoudi, Y. H. Teow, and A. W. Mohammad. 2016. Preparation of Novel Polysulfone-Fe₃O₄/GO Mixed-Matrix Membrane for Humic Acid Rejection. *Journal of Water Process Engineering*.
- [19] Mahmoudi, E., L. Y. Ng, M. M. Ba-Abbad, and A. W. Mohammad. 2015. Novel Nanohybrid Polysulfone Membrane Embedded with Silver Nanoparticles on Graphene Oxide Nanoplates. *Chemical Engineering Journal*. 277: 1-10.
- [20] Deng, J.-H., X.-R. Zhang, G.-M. Zeng, J.-L. Gong, Q.-Y. Niu, and J. Liang. 2013. Simultaneous Removal of Cd(II) And Ionic Dyes from Aqueous Solution using Magnetic Graphene Oxide Nanocomposite as an Adsorbent. *Chemical Engineering Journal*. 226: 189-200.
- [21] Basri, H., A.F. Ismail, and M. Aziz. 2012. Microstructure and Anti-Adhesion Properties Of PES/TAP/Ag Hybrid Ultrafiltration Membrane. *Desalination*. 287: 71-77.
- [22] Li, J.-F., Z.-L. Xu, H. Yang, L.-Y. Yu, and M. Liu. 2009. Effect of TiO₂ Nanoparticles on the Surface Morphology and Performance of Microporous PES Membrane. *Applied Surface Science*. 255 (9): 4725-4732.
- [23] Yu, L., Y. Zhang, B. Zhang, J. Liu, H. Zhang, and C. Song. 2013. Preparation and Characterization of HPEI-GO/PES Ultrafiltration Membrane with Antifouling and Antibacterial Properties. *Journal of Membrane Science*. 447: 452-462.
- [24] Zhang, M., M. Jia, and Y. Jin. 2012. Fe₃O₄/Reduced Graphene Oxide Nanocomposite as High Performance Anode for Lithium Ion Batteries. *Applied Surface Science*. 261: 298-305.
- [25] Shen, X., J. Wu, S. Bai, and H. Zhou. 2010. One-Pot Solvothermal Syntheses and Magnetic Properties of Graphene-Based Magnetic Nanocomposites. *Journal of Alloys and Compounds*. 506(1): 136-140.
- [26] Qi, T., J. Jiang, H. Chen, H. Wan, L. Miao, and L. Zhang. 2013. Synergistic Effect of Fe₃O₄/Reduced Graphene Oxide Nanocomposites for Supercapacitors with Good Cycling Life. *Electrochimica Acta*. 114: 674-680.
- [27] Kassaei, M. Z., E. Motamedi, and M. Majidi. 2011. Magnetic Fe₃O₄-Graphene Oxide/Polystyrene: Fabrication and Characterization of a Promising Nanocomposite. *Chemical Engineering Journal*. 172 (1): 540-549.
- [28] Safarpour, M., A. Khataee, and V. Vatanpour. 2015. Effect of Reduced Graphene Oxide/TiO₂ Nanocomposite with Different Molar Ratios on the Performance of PVDF Ultrafiltration Membranes. *Separation and Purification Technology*. 140: 32-42.
- [29] Wang, Z., H. Yu, J. Xia, F. Zhang, F. Li, Y. Xia, and Y. Li. 2012. Novel GO-Blended PVDF uUltrafiltration Membranes. *Desalination*. 299: 50-54.
- [30] Vatanpour, V., S.S. Madaeni, R. Moradian, S. Zinadini, and B. Astinchap. 2011. Fabrication and Characterization of Novel Antifouling Nanofiltration Membrane Prepared from Oxidized Multiwalled Carbon Nanotube/Polyethersulfone Nanocomposite. *Journal of Membrane Science*. 375(1-2): 284-294.
- [31] Rahimpour, A., M. Jahanshahi, S. Khalili, A. Mollahosseini, A. Zirepour, and B. Rajaeian. 2012. Novel Functionalized Carbon Nanotubes for Improving the Surface Properties and Performance of Polyethersulfone (PES) Membrane. *Desalination*. 286: 99-107.
- [32] Esfahani, M. R., J. L. Tyler, H. A. Stretz, and M. J. M. Wells. 2015. Effects of a Dual Nanofiller, Nano-TiO₂ and MWCNT, for Polysulfone-Based Nanocomposite Membranes for Water Purification. *Desalination*. 372: 47-56.